J Biochem Tech (2018) Special Issue (2): 163-168
ISSN: 0974-2328

Effect of Modifying Collector Voltage, Flow Rate and Distance on morphology of Silk Fibroin Nanofibers as tissue Scaffold

Amirasad Pourabadeh, Mohammad Mirjalili*, Mohammad Shahvazian

Received: 23 March 2018 / Received in revised form: 06 July 2018, Accepted: 13 July 2018, Published online: 05 September 2018

Abstract

Silk fibroin (SF) nanofiber scaffolds were made by electrospinning of fibroin fibers. Fibroin is a natural polymer with tremendous potential as a matrix for tissue engineering. Pure silk fibroin protein was extracted from Bombyx mori silk cocoon by degumming method using aqueous Na_2CO_3 solution followed by solubilizing in $CaCl_2$-C_2H_5OH-H_2O aqueous solution and frozen in liquid nitrogen, then lyophilized in freeze-dryer. The electrospinning of SF sponge was performed with formic acid, as a spinning solvent, at 7% (w/w) fibroin concentration. SF fibers with diameters down to the nanometer range, or nanofibers, are formed by subjecting a fluid jet to a high electric field. In this regard, voltage, flow rate and distance were used as variable parameters and effect of changes in these parameters were investigated. The morphology of SF nanofibers were characterized by scanning electron microscopy (SEM) at different magnification. After find the optimum parameters for electrospinning of SF nano fibers, Fibroblast L-929 cell line derived from normal subcutaneous areolar adipose tissue of mouse were cultured, expanded and seeded on selected electrospun SF nanofibers. Adhesion and proliferation of fibroblasts were investigated by MTT assay which showed no cytotoxicity and good choice for tissue engineering scaffold.

Key words: Silk Fibroin, Electrospinning, Nanofiber, Cell culture, Tissue engineering

Introduction

Nanofibers, which mimic collagen fibrils in the extracellular matrix (ECM), can be prepared from a host of natural and synthetic biomaterials and have multiple properties that may be beneficial to field of materials for medical applications. These properties include a large surface-area-to-volume ratio, high porosity, improved cell adherence, proliferation and migration, and controlled in vivo degradation rates. The large surface area of nanofiber mats allows for increased interaction with compounds and provides a mechanism for sustained release of antibiotics, analgesics, or growth factors into injured tissue; high porosity allows diffusion of nutrients and waste. Improved cell function on these scaffolds will promote healing (Hromadka et al., 2008). All the mentioned properties can be influenced by fiber morphology and diameter (Min et al., 2004; Kim et al., 2003). Those fiber morphology and diameter are depend on many parameters which can be divided into four main categories: polymer properties (molecular weight and solubility), polymer solution parameters (polymer concentration, solution viscosity, conductivity, surface tension, and etc.), processing conditions (applied voltage, nozzle-collector distance and feed rate), and ambient parameters (temperature, atmosphere pressure, and relative humidity) (Nasouri et al., 2012).

Silk fibroin, derived from silkworm cocoons, has attracted the scientific community due to its good biocompatibility along with suitable mechanical property. Fibroin protein is the major constituent 75 % of the cocoon and the remaining 25 % is sericin protein (Kim et al., 2005; Chirila et al., 2013). The molecular orientation makes this protein form a semi-crystalline structure which contains two phases: highly crystalline antiparallel β-sheet structure and non-crystalline part (Wang et al., 2004). The crystalline part lead to increase the strength and toughness and the non-crystalline part contributes the flexibility and elasticity to the fiber (Jin et al., 2005). Over the past years, many studies have explored silk fibroin in various forms from its regenerated solution, including porous scaffolds, films and electrospun fibers (Wharram et al., 2010).

Electrospinning is technique used to create micro and nanostructures that serve as microenvironments for cells to adhere and proliferate. The electrospun silk fibers with uniform micro or nano scale fibers have found utility in producing different biomaterials like wound dressing or scaffolds for a variety of biological applications such as bone, nerve and skin tissue (Valenzuela et al., 2012).

In this study, SF solutions have been used to electrospun polymer fibers of 50–750 nm diameter, and three parameters of processing

Amirasad Pourabadeh, Mohammad Mirjalili*, Mohammad Shahvazian
Department of Textile and Polymer Engineering, Yazd Branch, Islamic Azad University, P.O. Box 8916871967, Yazd, Iran.

***Email:** Dr.m.mirjalili@iauyazd. ac.ir

conditions including applied voltage, nozzle-collector distance and feed rate of SF electrospinning were investigated. We examined the morphology effect of the SF nanofiber by SEM images to be applied as a potential scaffold.

Experimental Methods

Preparation of Fibroin

Silk fibers are obtained from Bombyx Mori silkworm cocoons were washed twice with distilled water. In order to remove sericin coating from silk fibers, 10 g of silk in 2 L of a 0.02 M solution of Na2SO3 in distilled water were boiled for 30 min (Rockwood et al., 2011; Lammel et al., 2010), then the degummed fibers were washed thoroughly. Fibers were allowed to dry in a flow cabin. Silk fibers were solubilized in CaCl2-C2H5OH-H2O=1:2:8 (molar ratio), for 6h at 75°C. The solution was taken in a stirrer/hot plate at 60 RPM and was strained to remove the not dissolved fibers. CaCl2 was removed in a stirred cell for 7 h (Stirred Cell Model 8010, Amicon, Merck KGaA, Darmstadt, Germany) using a membrane disc of ultracel regenerated cellulose of 100 kDa (Merck KGaA, Darmstadt, Germany). The SF solution were instantaneously frozen in liquid nitrogen (-196 °C) and then lyophilized for 24 hours in a Liobras® freeze-dryer (model L101, Brazil) to obtain SF sponge.

Electrospinning

The SF electrospinning solution was prepared by dissolving the SF sponge in 98% formic acid (98–100 %, Merck) and stirred at room temperature for 3 h to obtain complete dissolution. In the electrospinning process, the SF solutions were placed into the 2.5 mL syringe (18–G) with a stainless needle connected to a high voltage power supplier. Flow rate, distance and spinning voltage were selected in the range of 1–1.4 (cc/h), 9–13 (cm) and 21–29 (kV), respectively.

Cell Viability

L-929 cells were cultured in an incubator (5% CO_2, 37 °C). The cells were suspended in McCoy's 5A medium and supplemented with 10% Fetal Bovine Serum (FBS) and 1% Penicillin-Streptomycin, with the exception of transfection experiments, where cells were grown in complete media without antibiotics.

The toxicity of PAMAM-grafted SF nanofibers was measured using the MTT assay. The number of viable cells was assayed over a period of 14 days, with the assumption that any toxic effects would be manifested within that period of time. The MTT chromophore represents the number of viable cells by measuring the amount of formazan generated by the mitochondrial enzymes of metabolically active cells (T M., 1983). Thus, the number of viable cells, can be correlated with the absorbance at 540 nm (λ_{max}). To quantify L-929 cells viability, MTT (50 µL, 5 mg/mL PBS) was added to each well and the plate was incubated for 3 h at 37°C. After the MTT treatment, the plates were centrifuged at 800 × g for 5 min, the supernatant removed, and the pellet was washed once with PBS. An extraction buffer (250 µL, 20% SDS/50% DMF, pH 7.4) was added to each well, and the gels were kept at 37°C, overnight. After solubilization, each well was diluted 10-fold, and aliquoted into one column of 96-well plate. The absorbance was measured at 0, 2, 6, 9, and 14 days, using a microplate spectrophotometer (Molecular Devices), at 550 nm, with the extraction buffer as the blank.

Scanning Electron Microscopy (SEM)

The morphology of SF nanofibers scaffold was observed, using SEM (S-5700, Hitachi, Tokyo, Japan). The intact samples coated with gold for SEM witnessing. In the SEM photos, the fiber diameters were determined by means of Image J software and the results were given as the average diameter ± standard deviation.

Results and Discussion

Effect of Changes in the Applied Voltage

We observed that the difference between the applied voltage that would cause a polymer drop to become unstable and that which would cause it to become conical in shape is very small. Any further increase in voltage beyond a critical value leads to the ejection of a polymer jet from the apex of the cone. As clearly shown from SEM images in Fig 1, this critical value of applied voltage was 25 kV. A voltage that be weaker or stronger than this critical value will result in beaded morphologies or even inhibit polymer jet initiation. With an increase in the applied voltage, the nanofiber diameter increases. The increase in nanofiber diameter is attributed to a higher polymer mass of jet stretching in correlation to increased charge repulsion within the jet and a strong external electric field as a consequence of an increase in the applied voltage.

Table 1. Characteristic of samples with different voltage in electrospinning of fibroin

NO. / Parameter	1	2	3	4	5
Voltage (kV)	21	23	25	27	29
Flow rate (ml/h)	1	1	1	1	1
Distance (cm)	10	10	10	10	10

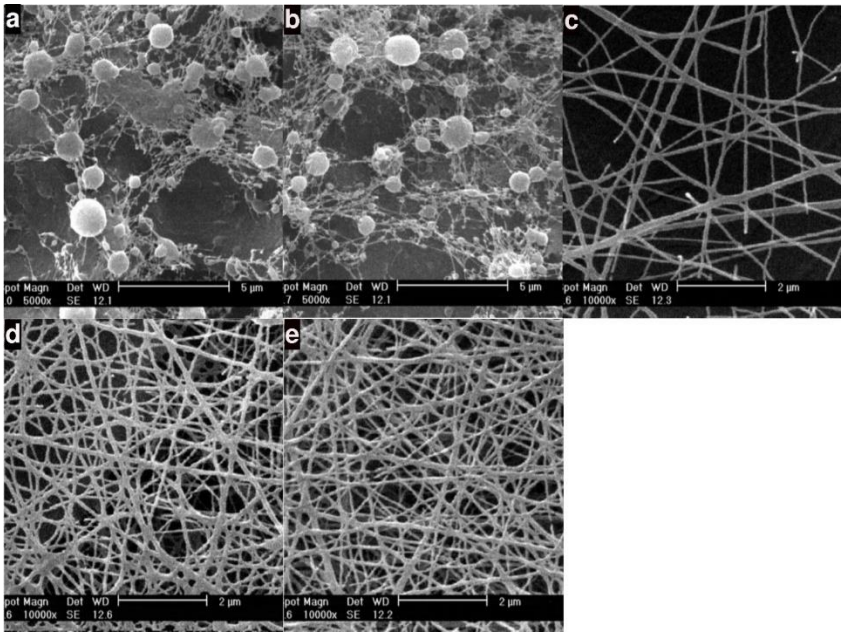

Figure 1. Morphologies of SF Nanofibers at Different voltage: a. 21; b. 23; c. 25; d. 27; e. 29 (kV).

Effect of changes in the Solution Flow-Rate

The flow-rate of the polymer solution through a capillary influences the nanofiber diameter, porosity, and geometry of the electrospun nanofibers. For the purpose of maintain the Taylor Cone shape at the capillary tip and avoid bead defects, a minimum flow-rate of the polymer is required in order to replace the solution that is lost when the nanofiber jet is ejected. As shown in Fig 2, the minimum flow-rate was 1.2 ml/h.

As the flow-rate increased, the available polymer volume was high which increased the nanofiber diameter. When the flow-rate was too high, the nanofibers were unable to dry completely before reaching the collector and higher bead defects were therefore observed. Flattened ribbon-like nanofiber morphology also result from incomplete drying of nanofibers due to a high flow-rate.

It was shown that the lower the solution flow-rate, the smaller the diameter of the resultant electrospun nanofibers and bead defects.

Table 2. Characteristic of samples with different flow rate in electrospinning of fibroin

NO. / Parameter	1	2	3	4	5
Voltage (kV)	27	27	27	27	27
Flow rate (ml/h)	1	1.1	1.2	1.3	1.4
Distance (cm)	10	10	10	10	10

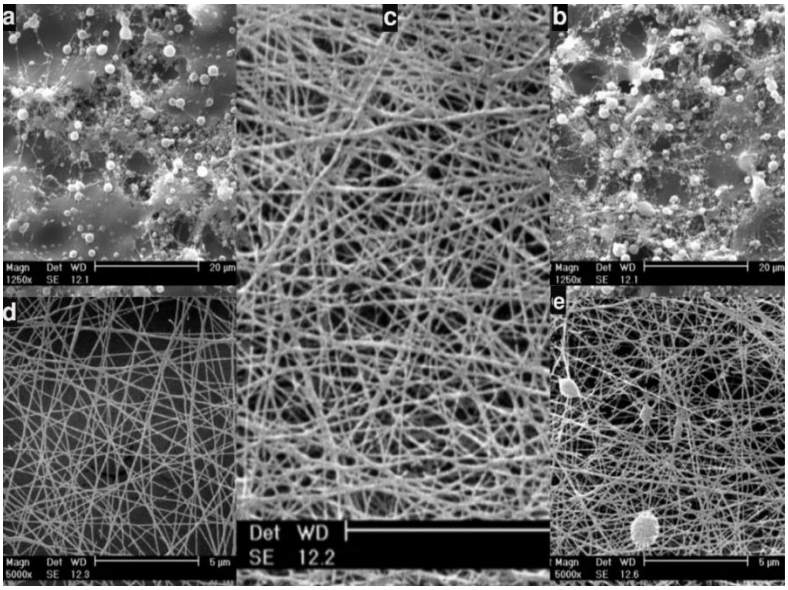

Figure 2. Morphologies of SF Nanofibers at Different Flow-Rate: a. 1.0; b. 1.1; c. 1.2; d. 1.3; e. 1.4 (ml/h).

Effect of changes in the Collector Distance

The capillary to collector distance influences the size and morphology of the nanofibers formed. However, its effect is relatively less profound compared to the other processing variables discussed. An optimum distance between the capillary and collector is desirable for nanofiber formation and on either side of this range bead formation or electro spraying instead of electrospinning may be observed.

Fig.3 shows the microstructure of SF electrospun at different Collector Distance. As shown in Figure 3, with an increase in the distance between the capillary and the collector the diameter of electrospun nanofibers decreases. At smaller distances the solvent does not have sufficient time to evaporate completely resulting in nanofibers with flattened structures due to inadequate drying. Also we observed an initiation of bead formation as the distance very decreased. These results clearly indicate that a decrease in nanofiber diameter with an increase in the distance up to 130 mm, beyond which the fiber jet became too small and unstable.

Table 3. Characteristic of samples with different distance in electrospinning of fibroin

NO. / Parameter	1	2	3	4	5
Voltage (kV)	27	27	27	27	27
Flow rate (ml/h)	1.2	1.2	1.2	1.2	1.2
Distance (cm)	9	10	11	12	13

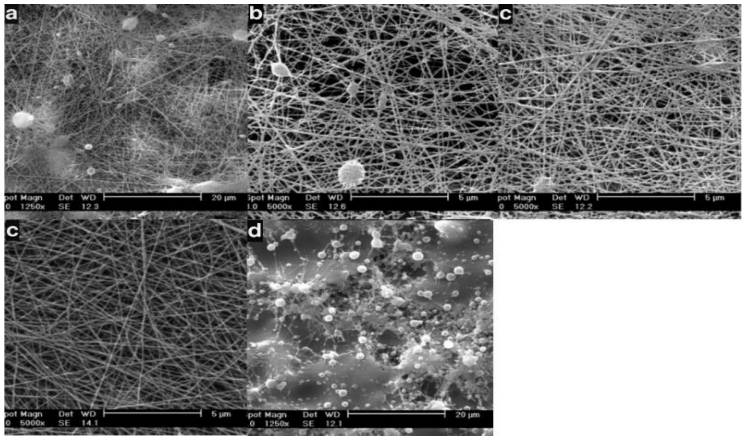

Figure 3. Morphologies of SF Nanofibers at Different Collector Distance: a. 9 cm; b. 10 cm; c. 11 cm; d. 12 cm; e. 13 cm.

MTT assay

After investigated the effect of changes in electrospinning parameters, we chose the optimum values of parameters and selected for MTT assay. Flow rate, distance and spinning voltage were selected in the values of 1.2 (ml/h), 12 (cm) and 27 (kV), respectively for optimum values. This selected SF nonofibers has the best morphology for use as a tissue engineering scaffold, because it has an appropriate three-dimensional structure with a porosity that is ideal for extracellular matrix and cell culture.

The response and cytotoxicity of modified fibroin scaffolds on L929 cells was investigated by the MTT assay. The MTT assay is based on the reduction of the yellow tetrazolium salt to purple formazan crystals, through dehydrogenase enzymes secreted from the mitochondria of metabolically active cells.

The amount of purple formazan crystals formed is proportional to the number of viable cells. A known concentration of cells was seeded onto fibroin scaffold. Figure 4 clearly indicates that the SF scaffold did not have any toxic effect on the L929 cells, and the percentage viability of the cells in the scaffolds and in control was at the same level of statistical significance. These results clearly indicate that SF-based scaffold are totally nontoxic to cells, and that the scaffold do not show any adverse effect on the growth of cells. Hence, these scaffold can be considered suitable for tissue engineering.

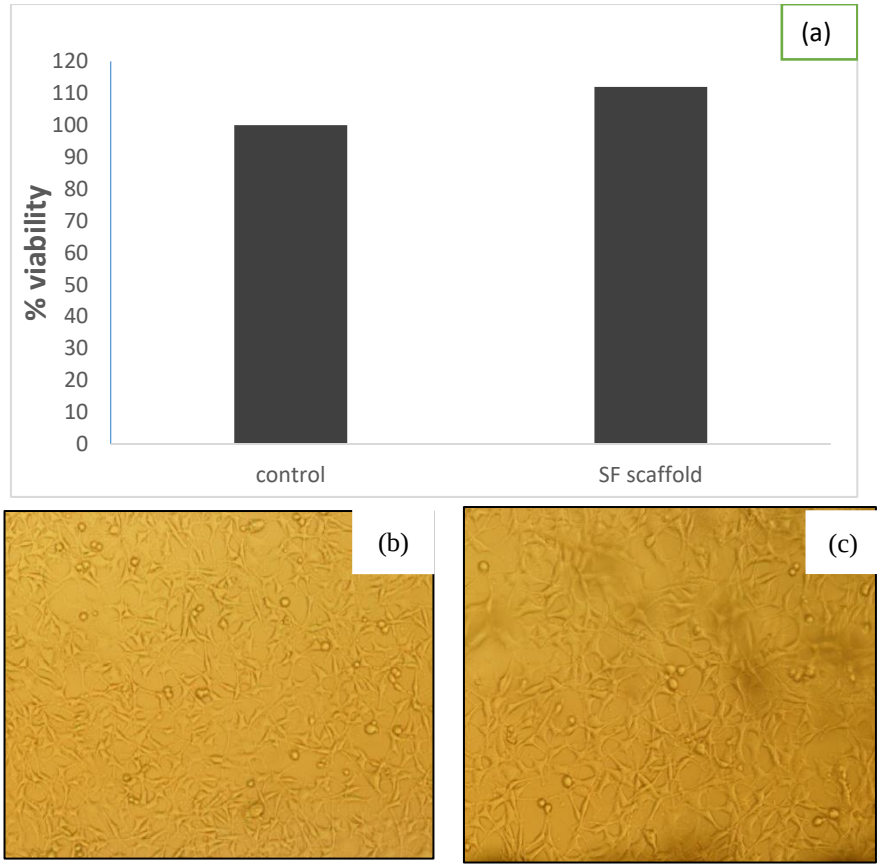

Figure 4. MTT Assays and Cytotoxicity Studies Against L-929 Cells: (a) Cell Viability (%) of L-929 Cells During 24h of Incubation, (b) Optical Microscopy Image of L-929 After Incubation with Control, (c) Optical Microscopy Image of L-929 After Incubation with SF Nanofibers Scaffold (c).

Conclusions

In this paper, Effect of Modifying Voltage, Rate and Distance on morphology of Silk Fibroin Nanofibers was investigated. As observed by SEM results to investigate the effect of increase in the applied voltage, the nanofiber diameter increases. The increase in nanofiber diameter is attributed to a higher polymer mass of jet stretching in correlation to increased charge repulsion within the jet and a strong external electric field as a consequence of an increase in the applied voltage.

As the flow-rate increased, the available polymer volume was high which increased the nanofiber diameter. This was attributed to the larger droplet at the end of the capillary, due to the very higher flow-rate, resulting in the solution having a faster trajectory and resulting in incomplete drying and the formation of bead defects. Also the lower the solution flow-rate, the smaller the diameter of the resultant electrospun nanofibers and bead defects.

With an increase in the distance between the capillary and the collector the nanofiber diameter initially decreased to a minimum and then increased. At smaller distances the solvent does not have sufficient time to evaporate completely resulting in nanofibers with formation of bead.

As shown by MTT assay which showed no cytotoxicity, fibroin nanofibers appears to be a probable choice for potential use in tissue engineering scaffold**.**

References

Chirila TV, Suzuki S, Bray LJ, Barnett NL, Harkin DG. Evaluation of silk sericin as a biomaterial: in vitro growth of human corneal limbal epithelial cells on Bombyx mori sericin membranes. Prog Biomater. 2013; 2:14.

Hromadka M, Collins JB, Reed C, Han L, Kolappa KK, Cairns BA, Andrady T, van Aalst JA. Nanofiber applications for burn care. J Burn Care Res. 2008; 29:695–703.

Jin H-J, Park J, Karageorgiou V, Kim U-J, Valluzzi R, Cebe P, Kaplan DL. Water-stable silk films with reduced β-sheet content. Adv Funct Mater. 2005; 15:1241–1247.

Kim HJ, Kim HS, Matsumoto A, Chin I-J, Jin H-J, Kaplan DL. Processing windows for forming silk fibroin biomaterials into a 3D porous matrix. Aust J Chem. 2005; 58:716–720.

Kim SH, Nam YS, Lee TS, Park WH. Silk fibroin nanofiber. Electrospinning, properties, and structure. Polym J. 2003; 35:185–190.

Lammel A.S, Hu X, Park S.H, Kaplan D.L, Scheibel T.R. Controlling silk fibroin particle features for drug delivery. Biomaterials. 2010; 31: 4583–4591.

Min B-M, Lee G, Kim SH, Nam YS, Lee TS, Park WH. Electrospinning of silk fibroin nanofibers and its effect on the adhesion and spreading of normal human keratinocytes and fibroblasts in vitro. Biomaterials. 2004; 25:1289–1297.

Nasouri K, Bahrambeygi H, Rabbi A, Shoushtari AM, Kaflou A. Modeling and optimization of electrospun PAN nanofiber diameter using response surface methodology and artificial neural networks. J Appl Polym Sci. 2012; 126:127–135.

Rockwood D.N, Preda R.C, Yucel T, Wang X, Lovett M.L, Kaplan D.L. Materials fabrication from Bombyx mori silk fibroin. Nat. Protoc. 2011; 6: 1612–1631.

T M. (1983). Rapid colorimetric assay for cellular growth and survival: Application to proliferation and cytotoxicity assays. Immunol Methods. 1983; 65: 55– 63.

Valenzuela F, Covarrubias C, Martínez C, Smith P, Díaz-Dosque M, Yazdani-Pedram M, Bellucci D, Sola A, Gentile P, Ciardelli G, et al. Bionanocomposites based on hydroxyapatite and bioactive glass nanoparticles. J Biomed Mater Res B Appl Biomater. 2012; 100:1387–1396.

Wang M, Jin H-J, Kaplan DL, Rutledge GC. Mechanical properties of electrospun silk fibers. Macromolecules. 2004; 37:6856–6864.

Wharram SE, Zhang X, Kaplan DL, McCarthy SP. Electrospun silk material systems for wound healing. Macromol Biosci. 2010; 10:246–257.